Final technical report for: Insertional Mutagenesis of *Brachypodium distachyon* DE-AI02-07ER64452

Abstract

Several bioenergy grasses are poised to become a major source of energy in the United States. Despite their increasing importance, we know little about the basic biology underlying the traits that control the utility of grasses as energy crops. Better knowledge of grass biology (e.g. identification of the genes that control cell wall composition, plant architecture, cell size, cell division, reproduction, nutrient uptake, carbon flux, etc.) could be used to design rational strategies for crop improvement and shorten the time required to domesticate these species. The use of an appropriate model system is an efficient way to gain this knowledge. *Brachypodium distachyon* is a small annual grass with all the attributes needed to be a modern model organism including simple growth requirements, fast generation time, small stature, small genome size and self-fertility. These attributes led to the recommendation in the DOE's "Breaking the Biological Barriers to Cellulosic Ethanol: A Joint Research Agenda" report to propose developing and using *B. distachyon* as a model for energy crops to accelerate their domestication. Strategic investments (e.g. genome sequencing) in *B. distachyon* by the DOE are now bearing fruit and *B. distachyon* is being used as a model grass by hundreds of laboratories worldwide. Sequence indexed insertional mutants are an extremely powerful tool for both forward and reverse genetics. They allow researchers to order mutants in any gene tagged in the collection by simply emailing a request. The goal of this project was to create a collection of sequence indexed insertional mutants (T-DNA lines) for the model grass *Brachypodium distachyon* in order to facilitate research by the scientific community. During the course of this grant we created a collection of 23,649 *B. distachyon* T-DNA lines and identified 26,112 unique insertion sites. The collection can be queried through the project website (http://jgi.doe.gov/our-science/science-programs/plant-genomics/brachypodium/brachypodium-t-dna-collection/) and through the Phytozome genome browser (http://phytozome.jgi.doe.gov/pz/portal.html). The collection has been heavily utilized by the research community and, as of October 23, 2015, 223 orders for 12,069 seeds packets have been filled. In addition to creating this resource, we also optimized methods for transformation and sequencing DNA flanking insertion sites.

Accomplishments

Our results can be broken into four areas: **1)** Creating a collection of *Brachypodium distachyon* T-DNA mutants **2)** Sequencing DNA flanking the insertion sites to determine the position of the T-DNA in the genome **3)** Validating the collection **4)** Data access and seed distribution

1) Creating a collection of *Brachypodium distachyon* T-DNA mutants

During the course of this grant we created 23,649 fertile T-DNA lines. Along the way, we increased transformation efficiency through optimization of the tissue culture conditions and the T-DNA vector. At the time we proposed this project *B. distachyon* was already one of, if not the, most efficiently transformed grass(es). Nevertheless, transformation requires numerous tissue culture steps and is therefore labor intensive. In order to maximize the number of T-DNA lines produced during the course of this grant we continually optimized the transformation method with an eye toward reducing the labor and cost per T-DNA line generated. The greatest

improvement came from eliminating an entire subculture step: placing callus onto recovery media with no selective agent after co-cultivation with *Agrobacterium*. In addition to the labor and time saved by eliminating a transfer and one week of incubation, this improvement increased the efficiency of subsequent steps because it reduced the growth of non-transgenic callus that occurred on the recovery media. We also began moving callus onto regeneration media sooner and discarding callus that had not regenerated plants by 4 weeks. These improvements decreased labor and growth chamber space required per transgenic line created. These results were presented in our initial description of the T-DNA collection (Bragg, Wu et al. 2012) and in four book chapters (Vogel and Bragg 2009, Bragg, Ludmila et al. 2010, Bragg, Anderton et al. 2015, Hsia and Vogel 2015).

Another avenue we explored to improve efficiency was to evaluate new inbred lines for transformability. We examined the tissue culture performance of a portion of a large collection of 187 inbred lines we characterized (Filiz, Ozdemir et al. 2009, Vogel, Tuna et al. 2009). We did identify lines that regenerated much better than our standard line, Bd21-3 (Fig. 1). However, since these lines flowered later and required longer vernalization to induce flowering we did not used them to generate T-DNA lines.

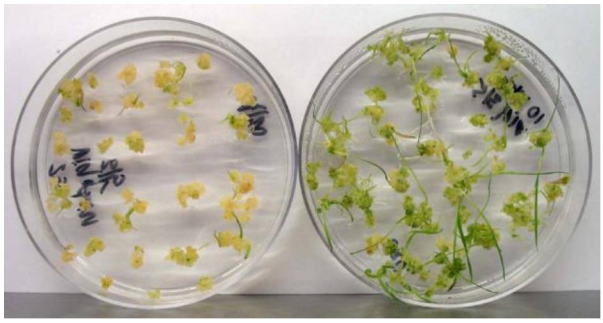

Adi3 Adi9

Figure 1. Tissue culture performance of new inbred lines. In an effort to find a more efficient line for transformation, we evaluated new inbred lines for callus formation and regeneration, the limiting steps in transformation. While we found lines with superior regeneration rates, they required more vernalization than our standard line (Bd21-3). Thus, we did not switch to the new lines for mutagenesis. Note that callus from Adi9 has many more shoots than callus from line Adi13.

Vector optimization

Hand in hand with our transformation method improvements, we altered different features in our vectors to improve transformation efficiency and success at obtaining sequence flanking regions adjacent to the T-DNA insertions. The largest improvement came from switching to a maize ubiquitin promoter to drive the selectable marker. This improved transformation efficiency to 50%, from 30 to 44%, when compared to the CaMV35S promoter we were using (Fig. 2 A) (Bragg, Wu et al. 2012). We also tested the rice actin and tubulin promoters, but found both to work poorly. In addition, we compared glufosinate and hygromycin as selective agents. In this case, we found that glufosinate selection was not as efficient as hygromycin because glufosinate did not kill non-transgenic callus as cleanly as hygromycin. This made it harder to select transgenic callus which led to more non-transgenic escapes (Fig. 2 B). Thus, we chose to use hygromycin as the selectable marker for the creation of the T-DNA collection. However, we still needed a second selectable marker to transform T-DNA lines that are already resistant to hygromycin. This is particularly important for complementing mutants with a wild type version of a gene to definitively assign function to the gene in question. We tested *nptII* as a resistance gene for the antibiotic paromomycin. We used paromomycin because most grasses are naturally resistant to kanamycin. We were able to efficiently transform *B. distachyon* using *nptII* as a selectable marker (Bragg, Anderton et al. 2015). To demonstrate the utility of paromomycin selection, we

complemented a mutant with a T-DNA construct containing *nptII* as the selectable marker (Figure 3).

A

Construct	pOL001	pJJ2LB
promoter driving Hyg gene	35S with intron	maize ubiquitin
# callus pieces	1037	991
# regenerants	334	476
# survive in soil	313	439
transformation efficiency (%)	30	44

B

Construct:	pJJ2LB	UbiBAR
selectable marker	Hyg	BAR
# regenerants	54	77
# survive in soil	51	34
% surviving	94	44

Figure 2. T-DNA vector optimization. **(A)** Using the maize ubiquitin promoter to drive the hygromycin resistance gene greatly improved transformation efficiency. The table summarizes results from six transformations comparing vectors pOL001 and pJJ2LB. Transformation efficiency (# transgenic plants surviving in soil / # callus pieces transformed) is 47% higher with the maize ubiquitin promoter than with the CaMV35S promoter. We also compared rice actin and rice tubulin promoters driving the hygromycin resistance gene and saw low transformation efficiency (not shown). **(B)** Hygromycin selection is more efficient than Basta selection. Results of side-by-side transformation with vectors that differ in selectable markers. Note that the survival of plantlets after moving to soil is lower for Basta selection probably because they were not transgenic. Additionally, hygromycin selection was faster (3 weeks of selection rather than 5) and generated a larger number of transgenic plants. (C)

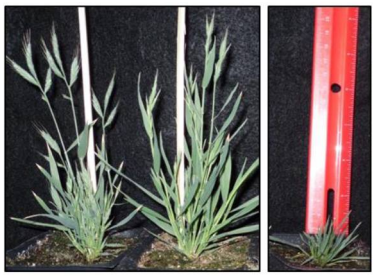

Figure 3. Complementation of a T-DNA mutant, *crk1*. To conclusively demonstrate that the phenotype observed in *crk1* was due to the T-DNA insertion, we introduced a wild-type version of *CRK1* into the T-DNA mutant. This required us to use a different selectable marker than was used to create the of the original T-DNA line. This was accomplished using *nptII* gene as the selectable marker and paromomycin as the selective agent.

2) Sequencing DNA flanking the insertion sites and determining the position of the T-DNAs in the genome

During the initial funding period of this grant we used inverse-PCR followed by Sanger sequencing to sequencing DNA flanking the T-DNA insertion sites. Using this approach we sequenced 7,145 mutants and identified 5,285 unique insertion sites as described in this publication (Bragg, Wu et al. 2012). However, while this approach was the state of the art at the time and it has been used to sequence many thousands of Arabidopsis T-DNA mutants, it suffers from two major limitations. First, it is very labor intensive because each line must be handled independently for DNA isolation, inverse PCR and sequencing. Second, if a given line contains more than one T-DNA insertion (the average number of T-DNA insertions per line is 1.5) the PCR products can interfere with each other during Sanger sequencing to produce unintelligible overlapping sequences. Fortunately, advances in next generation sequencing made it possible to solve both of these limitations. In collaboration with the Ecker lab at the SALK institute, we used

their TDNA-Seq method to sequence 23,156 T-DNA lines during the renewal portion of this grant. Figure 4 shows the work flow for the TDNA-Seq method. A key feature of this method is the multidimensional pooling that combines leaf samples from 10,000 plants into only 40 pools. Thus, instead of performing 10,000 DNA extractions it is only necessary to extract DNA from 40 pools. Likewise, instead of 10,000 PCR and Sanger sequencing reactions, only 40 Illumina sequencing libraries need to be made from 40 PCR reactions. These individual libraries can be barcoded and run together in a single Illumina run. This greatly reduces the labor, time and reagent costs. In addition, since individual DNA molecules are sequenced by Illumina, there is no interference when a line contains more than one T-DNA insertion. This is a rare instance where a new method is both cheaper and better. Using TDNA-Seq we sequenced 21,165 T-DNA lines and identified 21,078 insertion sites bringing the overall total number of unique insertion sites to 26,112 (Table 1).

We determined the location of the insertions sites with respect to genes using the JGI v2.1 annotation. The locations are summarized in Table 1. Significantly, 6,023 genes contain insertions in exons or introns and are thus likely to be null alleles. Another 1,107 genes may be knocked out by insertions in the 5'UTR. Thus, while this population is not saturated, 22% of the genes in the v2.1 annotation contain insertions in exons, introns or 5'UTRs.

Table 1. Distribution of insertion sites.

	No. of unique insertions[1]	Unique gene insertions[2]
Exon	3,769	3,401
intron	3,427	2,622
5' UTR	1,446	1,107
3' UTR	1,112	799
Near[3]	7,217	4,911
Intergenic	9,141	na
Total	26,112	12,840

[1]Tandem insertions within 500bp were counted as one insertion.

[2]Only one insertion was counted per gene. When multiple lines had insertions in the same gene, only the most useful insertions was counted (e.g. If there was an insertion in an exon and in an intron only the insertion in the exon was counted.)

[3]Insertions within 1,000 bp upstream or downstream of a gene (introns, exons, and UTRs).

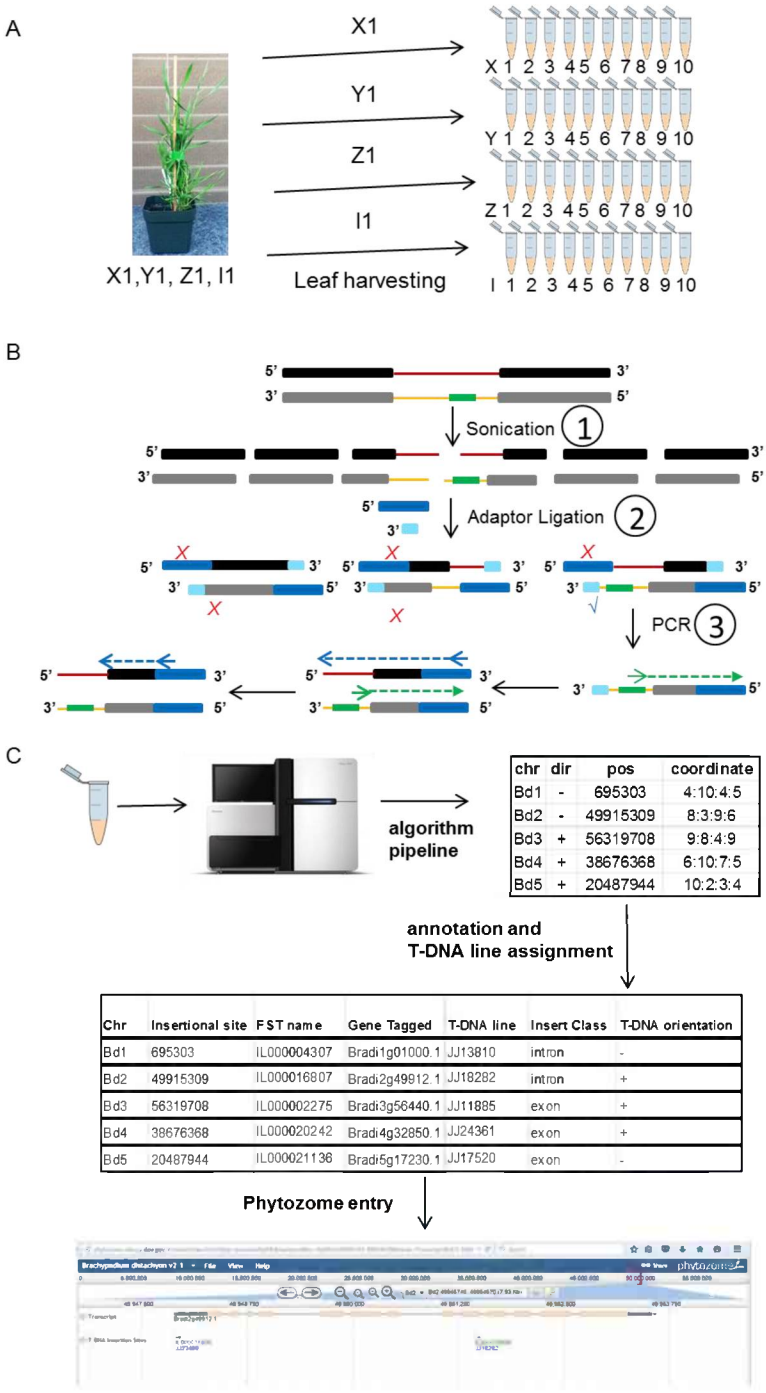

Figure 4. Project flowchart for Illumina sequencing of T-DNA insertions. (A) Four-dimensional pooling and tissue collection strategy. Each mutant is assigned four unique coordinates (x,y,z,i) that correspond to four of the 40 DNA pools represented by the tubes on the right. (B) The T-DNA insertion is represented by the thin colored lines and the genomic DNA by the thick gray/black bars. Generation of Illumina libraries organized into 3 steps, DNA sonication (①), adaptor ligation (②), and PCR amplification for enrichment of DNA region with T-DNA (③). T-DNA primer, green bar. 5' adaptor, blue bar. 3; adaptor, sky blue bar. Green arrow, T-DNA left border primer. Blue arrow, primer containing 5' adaptor sequences. (C) Sequencing and data analysis of 40 libraries using Illumina Hiseq and TDNA-Seq pipeline.

3) Validating the collection

We evaluated the quality and utility of the collection in two ways: validation of insertion sites and phenotypic characterization of select mutants. Since the TDNA-Seq method requires complex pooling and data deconvolution we used PCR to determine if there was an insertion where predicted for 146 predicted insertion sites (Table 2). For the second and third batches of mutants sequenced by TDNA-Seq a remarkable 98% of the insertions we examined were verified. The success rate for the first batch of mutants sequenced by TDNA-Seq was lower, 64%. The lower success rate is likely due to the fact that T1 or T2 plants segregating for the insertions were sampled. This required us to sample multiple plants for each line which greatly increased the complexity of sampling.

Table 2. Verification of insertion sites identified by TDNA-Seq.

Batch 1[1]			Batch 2+3		
total number of insertions	insertion sites tested	insertion sites verified (%)	total number of insertions	insertion sites tested	insertion sites verified (%)
3,670	42	27(64)	11,305	104	102(98)

[1]Batch one consisted of segregating plants samples at the T1 or T2 generation. Batch 2 and 3 plants were sampled at the T0 generation.

To demonstrate the utility of the collection we phenotypically characterized five lines with mutations in genes previously shown to have obvious phenotypes in other plants. In each case, the phenotype observed in the *B. distachyon* mutant was consistent with observations in other plants (Figures 5-9). This validates every step in the process from the creation of the lines to the assignment of insertion sites to specific genes to the display of data in Phytozome.

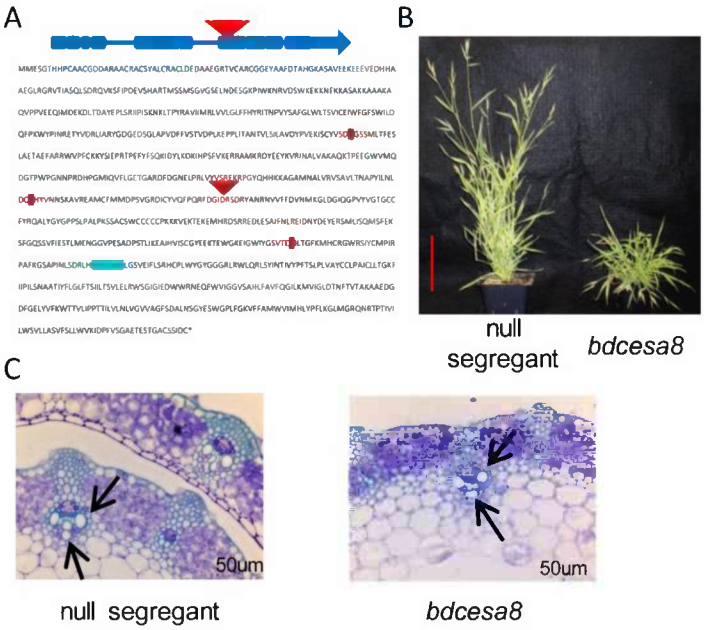

Figure 5. Phenotypic analysis of a mutant in *BdCESA8*, a putative cellulose biosynthetic gene. (A) T-DNA line JJ18282 contains an insertion in an exon of *Bradi2g49912* (inverted red triangle) within a conserved glycosol transferase domain that contains, three aspartic acid (D, in red) and the QxxRW motif (QVLRWA, in skyblue). (B) Images of 8-week old *bdcesa8* and its null segregant sibling. Red scale bar= 8cm. (C) Cross sections of mutant and null segregant stems stained with toluidine blue. Black arrows point at xylem cells. Note the irregular shape of the xylem cells in *bdcesa8*.

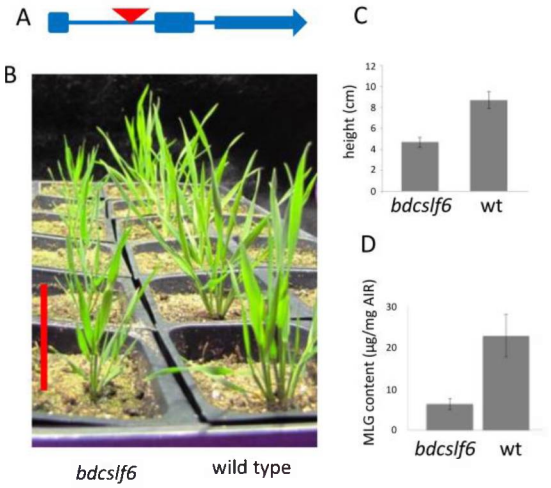

Figure 6. .Phenotypic analysis of a mutant in *BdCSLF6*, a glucosyltransferease required for mixed linkage glucan biosynthesis. (A) Graphic representation of the T-DNA insertion in the first intron of *Bradi3g1630.* (B) Visual appearance at 3-weeks-old. Scale bar=4cm. (C) Average height of 2-week old plants. (n=24, $p<0.005$). (D) Mixed linkage glucan content in seedlings. Error bars based on n=10.

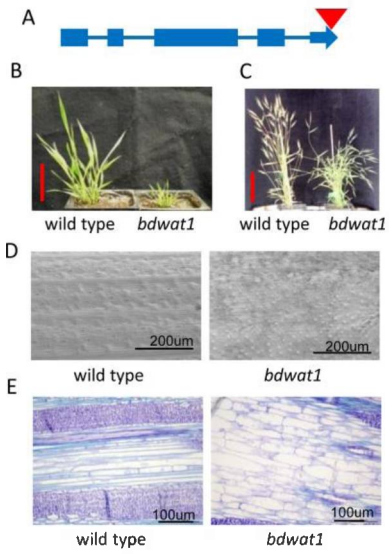

Figure 7. Phenotypic characterization of a mutation in the *B. distachyon* ortholog of the walls are thin 1, *WAT1*, gene which encodes a tonoplast protein required for normal secondary cell wall formation. (A) Illustration of the T-DNA insertion site in line JJ24092 in Bradi1g21860, *BdWAT1*. (**B**). Appearance of 3-weeks-old plants. Note the dwarf phenotype of *bdwat1*. Scale bar = 4cm (C) Appearance of 8 week old adult plants. Note that the development of *bdwat1*is delayed, but they eventually flower and make seed. Scale bar = 8cm. (D) Scanning electron microscope images of basal parts. Note the irregularly shaped cells in *bdwat1*. (E) Longitudinal section of toluidine stained stems. Note the irregularly shaped cells in *bdwat1* cells.

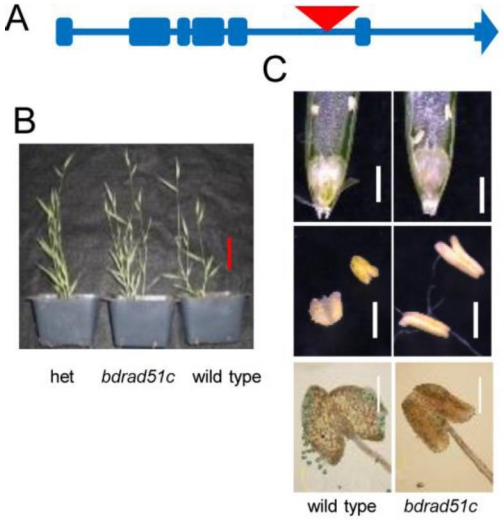

Figure 8. Phenotypic analysis of a mutant in the *B. distachyon* ortholog of *RAD51C,* a gene required for meiosis. (A) Illustration of the T-DNA insertion site in line CRC377. Note that the T-DNA has inserted into an intron in gene Bradi2g41710, *BdWAT1*. (B) Images of 4-week old hemizygous, homozygous mutant and wild type plants. Note that *bdrad51c* plants appear wild type. Red scale bar= 4cm. (C) *bdwat1* plants are male sterile. Top panel, dissected flowers showing shrunken anthers in *bdrad51c.* Scale bar = 1mm. Middle panel, anthers. Scale bar =1mm. Bottom panel, Alexender's dye stained anthers. Viable pollen stains blue. Scale bar = 200um. Note that *bdrad51c* does not produce viable pollen.

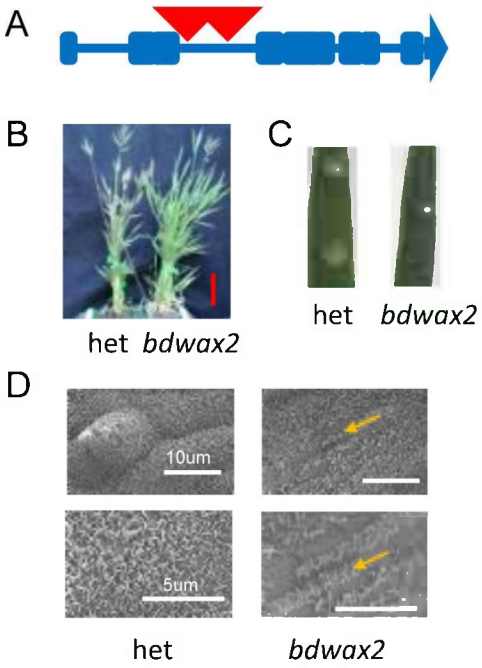

Figure 9. Phenotypic analysis a mutant in a wax biosynthesis gene, *BdWAX2*. (A) Illustration of the tandem T-DNA insertion sites in line JJ17731 into *Bradi3g48997, BdWAX2. (B)* Images of 5-weeks-old hemizygous and *bdwax2* plants. Scale bar=8cm. Hemizygous plants appear wild-type. (C) Images of water droplets on hemizygous and *bdwax2* leaves. Note that water does not beat on *bdwax2* due to decreased wax and hydrophobicity. (B) Scanning electron micrographs of hemizygous and *bdwax2* leaves. Note that *bdwax2* leaves have fewer wax crystals (arrows).

Activation tagging

The majority of the T-DNA lines (18,603 lines, 79%) were made with the activation tagging construct, pJJ2LBA (Bragg, Anderton et al. 2015). Activation tagging relies on a transcriptional enhancer on the T-DNA to stimulate overexpression of nearby genes (Hayashi, Czaja et al. 1992). This over expression can lead to gain of function mutants that are particularly useful for studying the function of functionally redundant or essential genes because traditional knockout mutants are not informative or lethal. To test the function of the 4X 35S enhancer found on the pJJ2LBA T-DNA, we used qRT-PCR to examine the expression of genes near the insertion site in three T-DNA mutants. In each case a nearby gene was expressed 2-10 fold higher in duplicate experiments indicating that the enhancer is working as expected (not shown). Given that the collection contains, on average, one T-DNA insertion every 10 kb and the enhancer can enhance expression up to at least 12kb away (Weigel, Ahn et al. 2000, Qu, Desai et al. 2008) the majority of *B. distachyon* genes are potential targets for activation tagging. Figure 10 presents a detailed characterization of one activation tagged mutant. In this example, we identified two independent activation mutants that both result in a dominant dwarf phenotype and both cause overexpression of the same nearby gene. Remarkably, a third T-DNA line contained an insertion in the same gene. This knockout line had no obvious phenotype suggesting genetic redundancy. This assertion was supported by the existence of a very closely related gene in *B. distachyon*. This particular example highlights the power of activation tagging to assign function to functionally redundant genes.

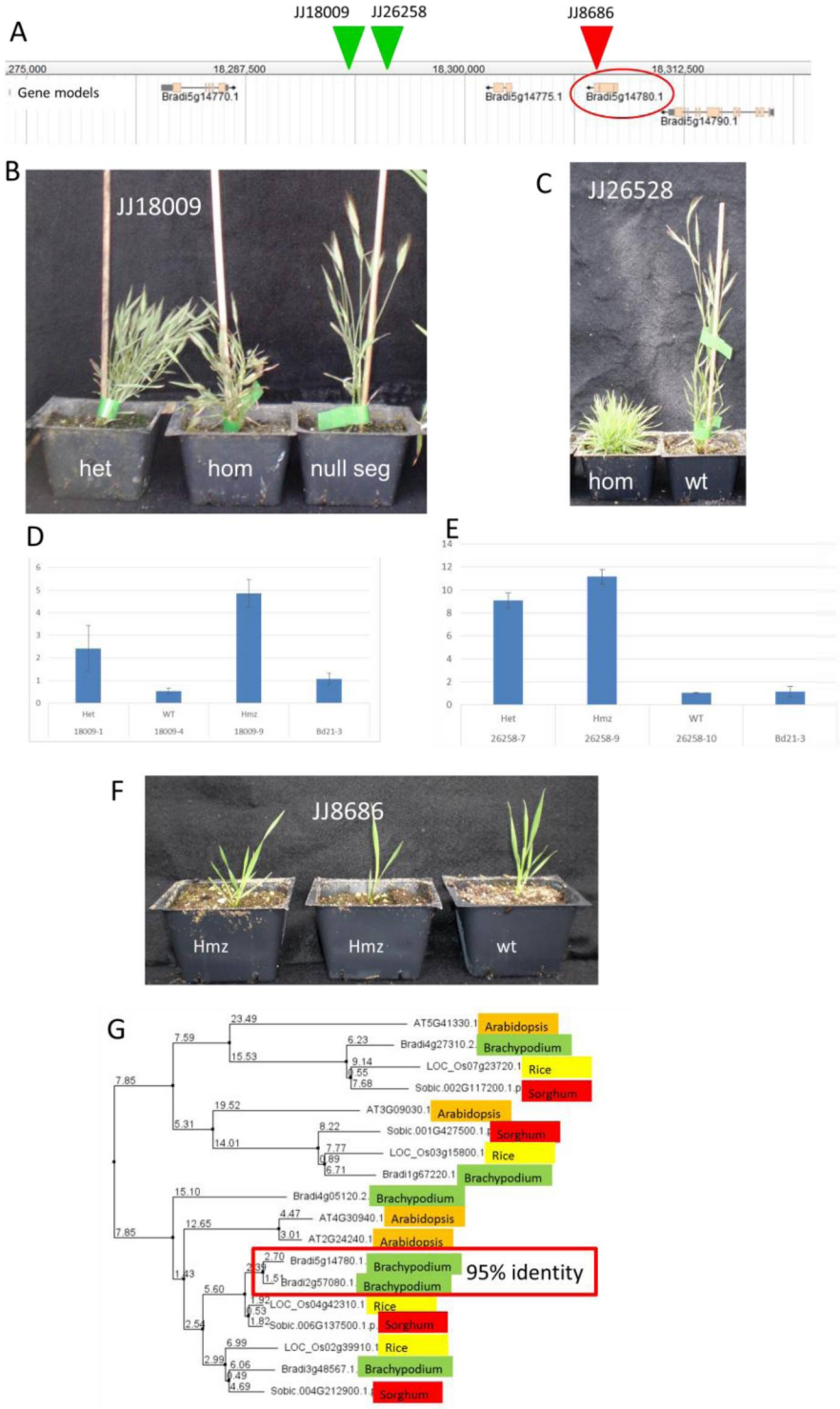

Figure 10. Activation tagging example. (A) Location of insertion sites for three T-DNA mutants. The green arrows indicate mutations that are enhancing expression of a nearby gene, Bradi5g14780, circled in red. The red arrow indicates the location of a T-DNA in the same gene. This is expected to knockout Bradi5g14780. (B) Adult phenotype of mutant JJ18009. Note that both heterozygous and homozygous mutants show a dwarf phenotype indicating dominant inheritance. (C) Mutant JJ26528 shows the same dominant phenotype. Heterozygous JJ26528 mutants are dwarf, but were not available for this photograph. (D and E) Both JJ18009 and JJ26528 greatly enhance expression of Bradi5g14780 when heterozygous or homozygous. (F) T-DNA line JJ8686 which contains an insertion in Bradi5g14780 has no obvious phenotype suggesting genetic redundancy. (G) Neighbor Joining tree of the Bradi5g14780 gene family from four species. Note that Bradi5g14780 appears to have been recently duplicated in *B. distachyon* suggesting that genetic redundancy may be responsible for the lack of a phenotype when Bradi5g14780 is knocked out. This highlights the power of activation tagging to assign function to redundant genes.

3) Data access and seed distribution

In order to provide the community with access to the T-DNA collection we created a project website (http://jgi.doe.gov/our-science/science-programs/plant-genomics/brachypodium/brachypodium-t-dna-collection/). This site provides details about the collection and instructions on how to order T-DNA lines. In addition, users can download an excel sheet that contains a complete list of all insertions sites, their relative positions with respect to genes, possible Arabidopsis and rice orthologs as well as PFAM, Panther, KOG, KEGG, and GO terms. In addition, the location of the insertion sites have been incorporated into the Phytozome database (http://phytozome.jgi.doe.gov) where they can be viewed as a jbrowse track.

Distribution of T-DNA lines has grown exponentially since the first seed were ordered in 2010 (Figure 11). This increase has been driven by the increasing as the number of T-DNA lines available and the increasing number of researchers using *B. distachyon*. As of October 23, 2015, 223 orders for 12,069 seeds packets have been filled. The huge demand for seed is a clear indication of the value of this resource to the research community.

Conclusion

During the course of this grant we created a large collection of T-DNA mutants, identified the insertion sites and made the information and seeds available to the research community. In addition, by characterizing a small number of mutants we demonstrated the quality and utility of this collection including the power of activation tagging to assign function to functionally redundant genes. The success of this project can be measured in two main ways: First, our collection contains insertions in about 20% of all *B. distachyon* genes. While not comprehensive, a mutant collection of this size will be extremely valuable to many researchers. Second, the number of lines distributed is a direct measurement of the value of this resource. We filled 223 orders for 12,069 lines which clearly demonstrates the huge demand for this resource by the research community.

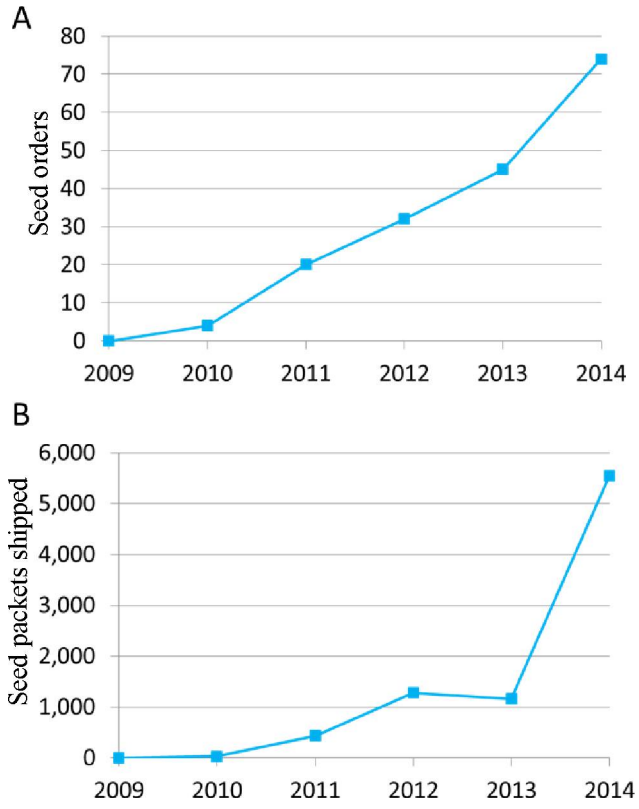

Figure 11. T-DNA seed distribution. (A) Number of seed orders shipped. (B) Number of lines shipped. Note the increasing demand as more lines become available.

Literature cited

Bragg, J. N., A. Anderton, R. Nieu and J. P. Vogel (2015). Brachypodium distachyon. Methods in Molecular Biology. **1223:** 17-33.

Bragg, J. N., T. Ludmila and J. P. Vogel (2010). Brachypodium distachyon, A Model for Bioenergy Grasses. Handbook of Bioenergy Crop Plants. C. Kole, C. P. Joshi and D. R. Shonnard. Boca Rotan, Taylor & Francis Group**:** in press.

Bragg, J. N., J. Wu, S. P. Gordon, M. E. Guttman, R. Thilmony, G. R. Lazo, Y. Q. Gu and J. P. Vogel (2012). "Generation and Characterization of the Western Regional Research Center Brachypodium T-DNA Insertional Mutant Collection." PLoS ONE 7(9): e41916.

Filiz, E., B. S. Ozdemir, F. Budak, J. P. Vogel, M. Tuna and H. Budak (2009). "Molecular, morphological, and cytological analysis of diverse *Brachypodium distachyon* inbred lines." Genome **52**(10): 876-890.

Hayashi, H., I. Czaja, H. Lubenow, J. Schell and R. Walden (1992). "Activation of a plant gene by T-DNA tagging: auxin-independent growth in vitro." Science **258**(5086): 1350-1353.

Hsia, M. M. and J. P. Vogel (2015). Transformation and T-DNA mutagenesis. Genetics and Genomics of Brachypodium. J. P. Vogel. Switzerland, Springer International Publishing. **18**.

Qu, S., A. Desai, R. Wing and V. Sundaresan (2008). "A versatile transposon-based activation tag vector system for functional genomics in cereals and other monocot plants." Plant Physiology **146**(1): 189-199.

Vogel, J. P. and J. N. Bragg (2009). *Brachypodium distachyon*, a New Model for the Triticeae. Genetics and Genomics of the Triticeae. C. Feuillet and G. Muehlbauer. New York, Springer. **7:** 427-449.

Vogel, J. P., M. Tuna, H. Budak, N. Huo, Y. Q. Gu and M. A. Steinwand (2009). "Development of SSR markers and analysis of diversity in Turkish populations of *Brachypodium distachyon*." BMC Plant Biology **9**: Art. No.: 88.

Weigel, D., J. H. Ahn, M. A. Blazquez, J. O. Borevitz, S. K. Christensen, C. Fankhauser, C. Ferrandiz, I. Kardailsky, E. J. Malancharuvil, M. M. Neff, J. T. Nguyen, S. Sato, Z. Y. Wang, Y. Xia, R. A. Dixon, M. J. Harrison, C. J. Lamb, M. F. Yanofsky and J. Chory (2000). "Activation tagging in Arabidopsis." Plant Physiol **122**(4): 1003-1013.

Training

Two post-doctoral fellows, and eight student interns worked on this project.

Publications and impact

Seed distribution

As of October 23, 2015 223 orders for 12,069 lines have been filled.

Publications (7)

Hsia, M. M. and J. P. Vogel (2015). Transformation and T-DNA mutagenesis. Genetics and Genomics of *Brachypodium*. J. P. Vogel. Switzerland, Springer International Publishing. **18** (in press).

Schneebeli, K., Mathesius, U., Zwart, A., **Vogel, J.P.**, Bragg, J., Watt, M., 2015 *Brachypodium distachyon* genotypes vary in resistance to *Rhizoctonia solani* anastomosis group 8. **Functional Plant Biology** (in press)

Bragg, N.B., Anderton, A., Nieu, R., and Vogel, J.P. 2015 *Brachypodium distachyon.* ***Agrobacterium*** **Protocols: Volume 1 (Methods in Molecular Biology vol. 1223)** Wang. K., New York, Springer. 2015, pp 17-33

Bragg, J.N., Wu, J., Gordon, S.P., Guttman, M.A., Thilmony, R.L., Lazo, G.R., Gu, Y.Q., **Vogel, J.P.** 2012 Generation and Characterization of the Western Regional Research Center *Brachypodium* T-DNA Insertional Mutant Collection **PLoS ONE** 7 (9) art. no. e41916

Brkljacic, J., Grotewold, E., Scholl, R., Mockler, T., Garvin, D.F., Vain, P., Brutnell, T., Sibout,R., Bevan, M., Budak, H., Caicedo, A.L., Gao, C., Gu, Y., Hazen, S.P., Holt, B.F., Hong, S.H., Jordan, M., Manzaneda, A.J., Mitchell-Olds, T., Mochida, K., Mur, A.J., Park, C.M., Sedbrook, J., Watt, M., Zheng, S.J. and **Vogel, J.P.** 2011. Brachypodium as a model for the grasses: Today and the future. **Plant Physiology** 157: 3-13

Tyler, L., Bragg, J.N., Wu, J., Yang, X., Tuskan, G.A., **Vogel, J.P.** 2010 Annotation and comparative analysis of the glycoside hydrolase genes in *Brachypodium distachyon.* **BMC Genomics** 11:600

Vogel, J. P. and J. N. Bragg (2009). *Brachypodium distachyon*, a New Model for the Triticeae. **Genetics and Genomics of the Triticeae**. C. Feuillet and G. Muehlbauer. New York, Springer. **7:** 427-449.

Manuscripts close to submission, all work completed manuscript written (1)

Hsia, M., O'Malley, R., Cartwright, A., Nieu, R., Gordon, S.P., Kelly, S., Williams, T., Wood, D.F., 1, Zhao, Y., Bragg, J.N., Jordan, M., Pauly, M., Ecker, J., Gu, Y.Q., **Vogel, J.P**., 2015 High throughput sequencing and functional validation of the JGI *Brachypodium distachyon* T-DNA Resource (manuscript is written and will be submitted as soon as a paper describing a technique used in work is submitted by collaborators)